

doi: 10.12029/gc20220604002

徐雯, 饶松, 王晓龙, 肖七林, 万泽鑫, 鲍一遥, 刘宇坤, 陶泽, 余家朝, 石湘, 程甜, 姜继连. 2025. 新疆吐哈盆地胜北洼陷中侏罗统超压发育与致密气成藏[J]. 中国地质, 52(2): 650–664.

Xu Wen, Rao Song, Wang Xiaolong, Xiao Qilin, Wan Zexin, Bao Yiyao, Liu Yukun, Tao Ze, She Jiachao, Shi Xiang, Cheng Tian, Jiang Jilian. 2025. Characteristics of Middle Jurassic overpressure and tight gas accumulation in Shengbei Sub-sag, Turpan-Hami Basin, Xinjiang[J]. Geology in China, 52(2): 650–664(in Chinese with English abstract).

## 新疆吐哈盆地胜北洼陷中侏罗统超压发育 与致密气成藏

徐雯<sup>1,2</sup>, 饶松<sup>1,2</sup>, 王晓龙<sup>1</sup>, 肖七林<sup>1</sup>, 万泽鑫<sup>1</sup>, 鲍一遥<sup>1</sup>, 刘宇坤<sup>3</sup>, 陶泽<sup>3</sup>,  
余家朝<sup>4</sup>, 石湘<sup>4</sup>, 程甜<sup>4</sup>, 姜继连<sup>4</sup>

(1. 长江大学油气资源与勘探技术教育部重点实验室, 湖北 武汉 430100; 2. 长江大学 地球科学学院, 湖北 武汉 430100; 3. 中国地质大学, 湖北 武汉 430074; 4. 中国石油吐哈油田分公司开发事业部, 新疆 哈密 839000)

**摘要:**【研究目的】吐哈盆地胜北洼陷致密气已成为拓展勘探新战场、发现新储量的重要领域, 致密储层发育特征及成藏机理已成为亟需解决的关键科学问题之一。【研究方法】运用地球化学、地球物理学和油气地质等综合研究方法, 对中侏罗统致密气源储特征和成藏期次进行了系统分析, 厘定了超压发育特征及对致密气成藏的控制作用。【研究结果】(1) 主力烃源岩的有机质类型以 III 型干酪根为主, 整体处于以生气为主的成熟期。中侏罗统发育低孔低渗—低孔特低渗致密储层, 平均孔隙度为 7.1%, 平均渗透率为  $0.074 \times 10^{-3} \mu\text{m}^2$ 。孔隙类型以次生溶蚀孔为主, 同时发育黏土矿物层间孔、黄铁矿晶间孔和微裂缝。(2) 中侏罗统发育以压力传导和生烃增压为成因的超压, 压力系数主要分布在 1.2~1.5, 纵向上超压顶界面位于七克台组中上部。超压主要分布在胜北洼陷东部和东南部, 断裂系统控制超压分布范围。(3) 烃源岩排烃持续时间较长, 从晚三叠世至今, 至少存在两期主要的天然气充注期, 两期主要成藏期次为: 晚侏罗世至早白垩世和古新世至今。【结论】中侏罗统致密气藏以“远源-近源两期成藏、压力-断裂协同输导、断裂-超压协调控制”的成藏模式为主。本文研究成果将为胜北洼陷致密气勘探开发提供科学依据和技术支持。

**关 键 词:**致密气; 超压与成因; 成藏期次; 油气勘查工程; 胜北洼陷; 吐哈盆地; 新疆

**创 新 点:**(1) 揭示胜北洼陷致密气成藏的源储特征, 超压与断裂系统相伴生, 控制生排烃和致密气充注;(2) 厘定了源储、超压(压力)、断裂等协同控制下的致密气成藏模式。

中图分类号: P618.13 文献标志码: A 文章编号: 1000-3657(2025)02-0650-15

## Characteristics of Middle Jurassic overpressure and tight gas accumulation in Shengbei Sub-sag, Turpan-Hami Basin, Xinjiang

XU Wen<sup>1,2</sup>, RAO Song<sup>1,2</sup>, WANG Xiaolong<sup>1</sup>, XIAO Qilin<sup>1</sup>, WAN Zexin<sup>1</sup>, BAO Yiyao<sup>1</sup>, LIU Yukun<sup>3</sup>,  
TAO Ze<sup>3</sup>, SHE Jiachao<sup>4</sup>, SHI Xiang<sup>4</sup>, CHENG Tian<sup>4</sup>, JIANG Jilian<sup>4</sup>

收稿日期: 2022-06-04; 改回日期: 2022-10-14

基金项目: 国家自然科学基金(41702135)和十四五前瞻性项目(2021DJ0405)联合资助。

作者简介: 徐雯, 女, 1986 年生, 硕士生, 主要从事石油地质与地热勘探方面的研究; E-mail: 475520992@qq.com。

通信作者: 王晓龙, 男, 1985 年生, 副教授, 主要从事地质与地球物理综合研究以及(非常规)油气地质方面的教学和研究工作; E-mail: wxlong@yangtzeu.edu.cn。

(1. Key Laboratory of Exploration Technologies for Oil and Gas Resources, Ministry of Education, Yangtze University, Wuhan 430100, Hubei, China; 2. School of Geosciences, Yangtze University, Wuhan 430100, Hubei, China; 3. Key Laboratory of Tectonics and Petroleum Resources, Ministry of Education, China University of Geosciences, Wuhan 430074, Hubei, China; 4. Development Division of PetroChina Tuha Oilfield Branch, Hami 839000, Xinjiang, China)

**Abstract:** This paper is the result of oil and gas exploration engineering.

**[Objective]** The tight gas in the Shengbei subsag of the Turpan–Hami Basin has become an important field for expanding new exploration battlefields and discovering new reserves. The development characteristics and accumulation mechanism of tight reservoirs have become one of the key scientific issues that need to be solved urgently. **[Methods]** Using comprehensive research methods such as geochemistry, geophysics and oil and gas geology, the characteristics and accumulation stages of tight gas sources and reservoirs in the Middle Jurassic were systematically analyzed, and characteristics of overpressure development and the controlling effect on tight gas accumulation were determined. **[Results]** (1) The organic matter type of the main source rocks is mainly type III kerogen, and the whole is in the mature stage dominated by gas generation. Middle Jurassic developed low porosity and low permeability–low porosity and ultra–low permeability tight reservoirs, with an average porosity of 7.1% and an average permeability of  $0.074 \times 10^{-3} \mu\text{m}^2$ . The pore type is dominated by secondary dissolution pores, while clay mineral interlayer pores, pyrite intercrystalline pores and micro–fractures are developed. (2) The Middle Jurassic developed overpressure caused by pressure conduction and hydrocarbon generation pressurization. The pressure coefficient was mainly distributed between 1.2 and 1.5. The overpressure top interface was located in the middle and upper part of the Qiketai Formation vertically. The overpressure is mainly distributed in the east and southeast of the Shengbei subsag, and the fault system controls the distribution range of the overpressure. (3) The hydrocarbon expulsion from source rocks lasted for a long time. From Late Triassic to the present, there have been at least two main periods of natural gas charging, and the two main accumulation periods are: Late Jurassic to Early Cretaceous and Paleocene to date. **[Conclusions]** The Middle Jurassic tight gas reservoirs are dominated by the accumulation model of "two–stage accumulation from far–source and near–source, pressure–fault coordinated transport, and fault–overpressure coordinated control". The research results in this paper will provide scientific basis and technical support for tight gas exploration and development in Shengbei Sub–sag.

**Key words:** tight gas; overpressure and origin; accumulation period; oil and gas exploration engineering; Shengbei Sub–sag; Turpan–Hami Basin; Xinjiang

**Highlights:** (1) Reveal the source rock and reservoir characteristics of tight gas accumulation in Shengbei Sub–sag, and overpressure is accompanied by fault system to control hydrocarbon generation and expulsion and tight gas charging; (2) Summarize the tight gas accumulation model under the cooperative control of source and reservoir, overpressure (pressure), fault, etc.

**About the first author:** XU Wen, female, born in 1986, master candidate, mainly engaged in petroleum geology and geothermal exploration research; E-mail: [475520992@qq.com](mailto:475520992@qq.com).

**About the corresponding author:** WANG Xiaolong, male, born in 1985, associate professor, mainly engaged in teaching and researching on integrated geology and geophysics and (unconventional) oil and gas geology; E-mail: [wxlong@yangtzeu.edu.cn](mailto:wxlong@yangtzeu.edu.cn).

**Fund support:** Supported by National Natural Science Foundation of China (No.41702135) and 14th Five–Year Forward–looking Projects (No.2021DJ0405).

## 1 引言

致密气勘探已成为非常规油气勘探非常重要的组成部分,致密砂岩储层成藏机理和主控因素的研究仍然是非常规油气地质学的基础性问题和重难点问题(赵靖舟等, 2013; 王朋等, 2020; Li et al., 2021; 曾凡成等, 2021)。在生烃、排烃、运移、聚集、成藏等过程中都发挥重要作用的超压系统(曹

华等, 2006; Li et al., 2021; Liu et al., 2021; Shi et al., 2013),广泛存在于含油气盆地沉积地层(Wang et al., 2019; Hua et al., 2021)。

吐哈盆地胜北洼陷非常规油气勘探证实致密砂岩气藏与超压相伴生,超压发育特征和成因、超压对致密气藏形成的贡献等问题是非常规油气高效勘探开发的难点和热点问题(曹华等, 2006; 郝爱胜等, 2021; Li et al., 2021)。本文基于地质、地震、

测井、地化等资料,对烃源岩和致密储层进行评价,对超压发育特征和成因进行分析,对致密气成藏期次进行厘定,探讨超压与致密砂岩气成藏的关系,为胜北洼陷致密气藏进一步勘探开发提供科学依据和技术支持。

## 2 区域地质概括

吐哈盆地位于西伯利亚、哈萨克斯坦和塔里木

三大板块的交接处,被喀拉乌山、博格达山、巴里坤山、哈尔力克山、觉罗塔格山等包围。整体呈长条状展布,地势表现为东高西低、北高南低(图 1a)。吐哈盆地进一步划分为 7 个二级构造单元,从西往东依次为:布尔加凸起、托克逊凹陷、台北凹陷、丁湖斜坡、了墩隆起、三堡凹陷和黄田凸起等([Zhao et al., 2010; Liu et al., 2011; 张品等, 2018; 荀红光等, 2019](#))。位于吐哈盆地北部的台北凹陷由胜北

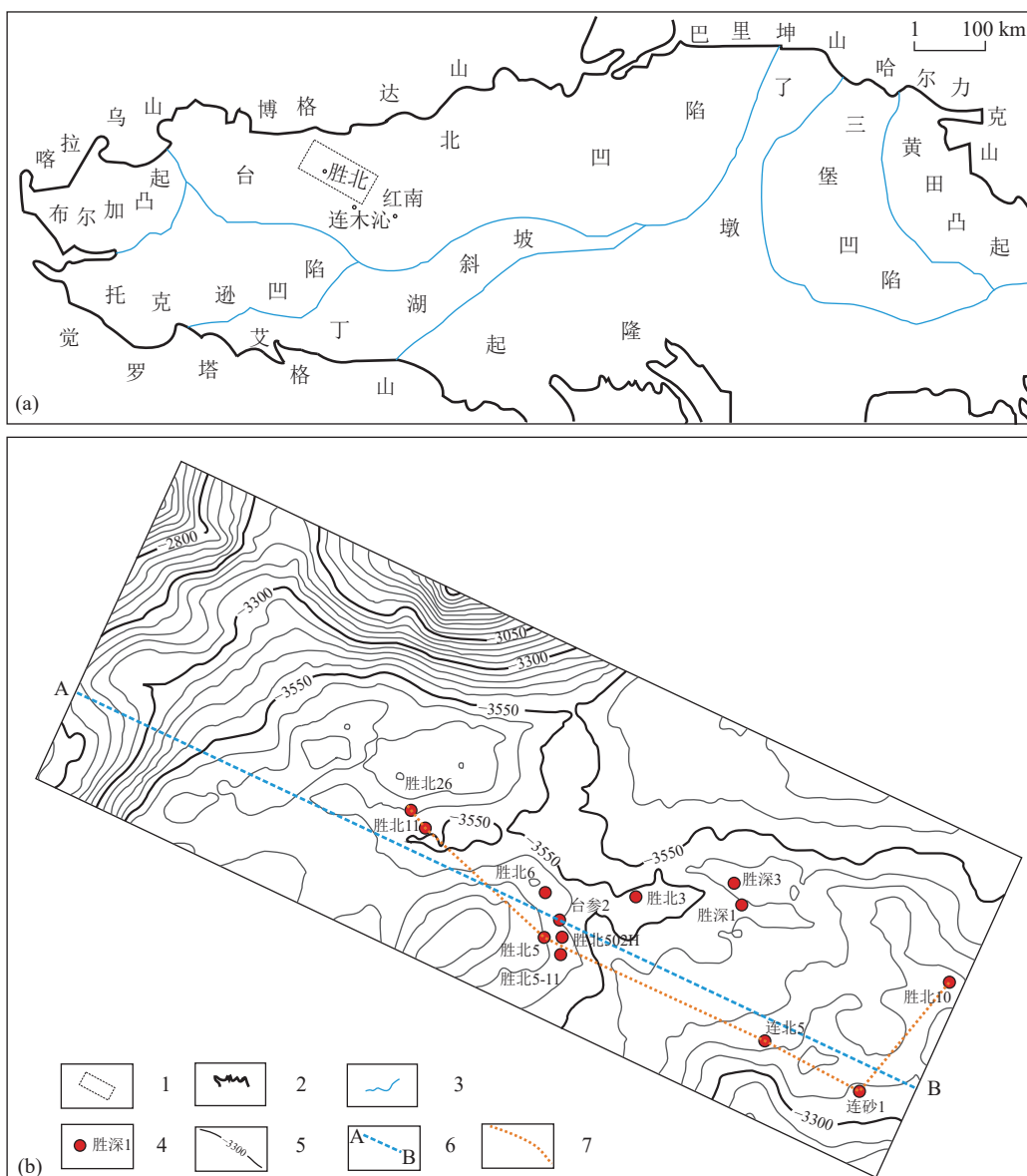


图 1 吐哈盆地构造单位划分图(a)、胜北洼陷等 T0 构造图(b)

1—研究区域; 2—盆地边界; 3—构造单元边界; 4—井名及井位; 5—等 T0 等值线; 6—地震剖面位置; 7—连井剖面位置

Fig.1 Division of tectonic units of Turpan-Hami Basin (a), T0 structural map of Shengbei Sub-sag (b)

1—Study area; 2—Basin boundary; 3—Structural unit boundary; 4—Well name and location; 5—Isoiline of T0; 6—Seismic profile position; 7—Well-connected profile location

洼陷、丘东洼陷和小草湖洼陷组成,位于台北凹陷西部的胜北洼陷是本文的研究区(图 1b)。

胜北洼陷主体发育低幅度构造,呈“洼中隆”构造格局,构造高点位于研究区北方。中侏罗统发育薄砂层致密储层,油气成藏条件好,气藏储量大(王劲松等,2009; 刘江涛等,2010; 唐文斌等,2017)。依据层序地层特征划分为七克台组、三间房组和西山窑组(图 2)。研究区现有胜北 26 井等 13 口探井揭示中侏罗世地层,七克台组以湖相泥岩为主,夹少量砂岩,中上部以暗色泥岩为主,下部

为灰色细砂岩、粉砂岩夹泥岩组合;三间房组上部地层以砂砾岩、细砂岩、粉砂岩及砂质泥岩与杂色泥岩组成的不等厚互层为主,中部以浅灰色砂岩夹杂色泥岩为主,底部以棕红色、紫红色泥岩为主;西山窑组上部以灰色块状砂岩、含砾砂岩为主,中部以浅灰色砂岩、碳质泥岩与煤互层为主,底部以灰色砂岩、含砾砂岩为主的含煤地层(杨占龙等,2005; 李红哲等,2006; 李在光等,2006a, b)。本文目的层位为中侏罗统七克台组、三间房组和西山窑组。

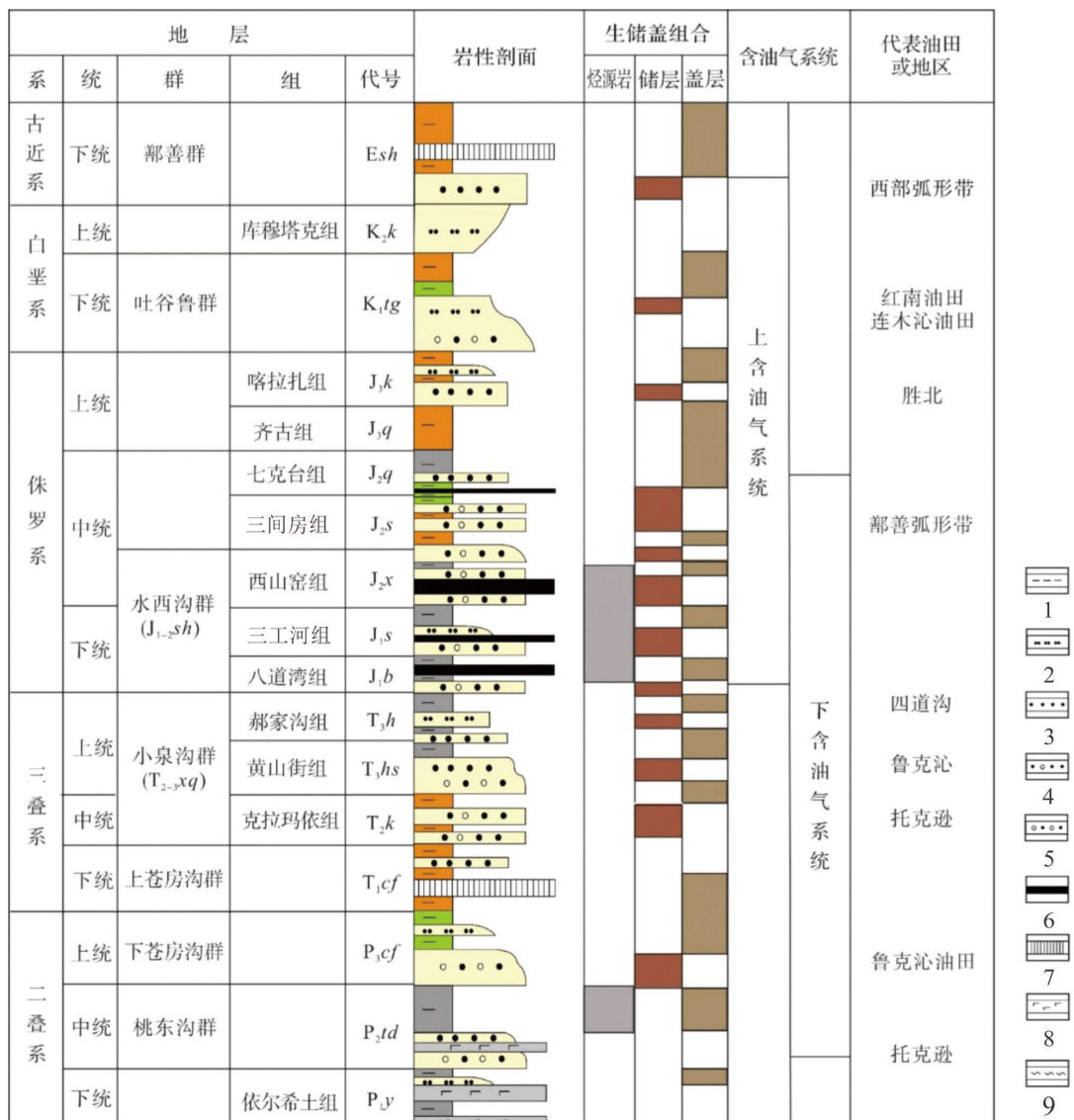


图 2 吐哈盆地地层综合柱状图(据苟红光等,2019)

1—泥岩;2—粉砂岩;3—砂岩;4—含粒砂岩;5—砾砂岩;6—煤;7—石膏层;8—玄武岩;9—凝灰岩

Fig.2 Comprehensive stratigraphic histogram of Turpan-Hami Basin (after Gou Hongguang et al., 2019)

1—Mudstone; 2—Siltstone; 3—Sandstone; 4—Grain-bearing sandstone; 5—Gravel sandstone; 6—Coal; 7—Gypsum layer; 8—Basalt; 9—Tuff

### 3 烃源岩与致密储层发育特征

胜北洼陷发育致密气藏, 中—下侏罗统发育七克台组湖相烃源岩、水西沟群煤系烃源岩, 中二叠统发育桃东沟群湖相烃源岩 (Wang et al., 2015; Wang et al., 2018; 荀红光等, 2019; Feng et al., 2020; 吴琰杰等, 2021; 李天军等, 2021)。本文主要采集揭示中下侏罗统的钻井岩心样品, 设计分析测试实验, 对烃源岩和储层进行评价分析。

#### 3.1 烃源岩评价

基于本次分析测试数据结合前人研究成果对研究区烃源岩进行评价(图 3a): 表明中—下侏罗统水西沟群(西山窑组、三工河组和八道湾组)有机质丰度优于中—上侏罗统(齐古组、七克台组和三间房组), 中—上侏罗统七克台组烃源岩丰度较高。因此, 研究区主力烃源岩为中—下侏罗统水西沟群、中侏罗统七克台组。同时已有勘探成果证实中

二叠统桃东沟群湖相烃源岩也为研究区主力烃源岩 (荀红光等, 2019; 李天军等, 2021; 吴琰杰等, 2021)。烃源岩热解最高峰温( $T_{\max}$ )与氢指数(HI)交汇图揭示侏罗统烃源岩氢指数普遍小于 200 mg/g, 烃源岩热解最高峰温主要分布在 435~450 °C, 有机质类型以 III 型干酪根为主(图 3b)。烃源岩镜质体反射率  $R_o$  与地层埋藏深度有较好的相关性(图 3c), 烃源岩镜质体反射率  $R_o$  值显示研究区烃源岩整体处于成熟期, 以生气为主。

#### 3.2 致密储层发育特征

物性数据显示研究区中侏罗统发育低孔低渗—特低渗致密储层, 具体特征如下(图 4a): 七克台组孔隙度范围在 4.06%~8.4%, 渗透率分布范围在  $0.003 \times 10^{-3} \sim 0.187 \times 10^{-3} \mu\text{m}^2$ ; 三间房组孔隙度分布范围在 3.8%~9.97%, 渗透率分布范围在  $0.001 \times 10^{-3} \sim 0.288 \times 10^{-3} \mu\text{m}^2$ ; 西山窑组孔隙度分布范围在 5.04%~9.95%, 渗透率分布范围在  $0.003 \times 10^{-3} \sim 0.288 \times 10^{-3} \mu\text{m}^2$ 。

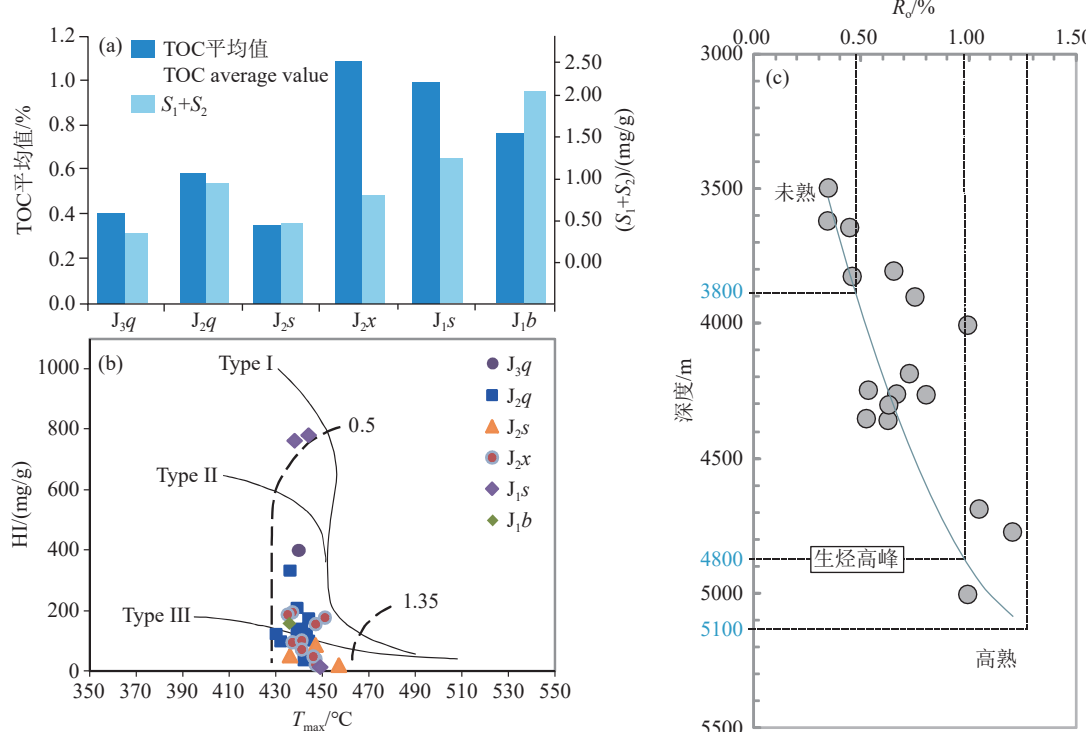


图 3 胜北洼陷侏罗系泥岩有机碳(a)和生烃潜量平均值分布直方图、烃源岩热解最高峰温和氢指数交汇图(b)、烃源岩镜质体反射率  $R_o$  与深度关系图(c)

$J_3q$ —齐古组;  $J_2q$ —七克台组;  $J_2s$ —三间房组;  $J_2x$ —西山窑组;  $J_1s$ —三工河组;  $J_1b$ —八道湾组

Fig.3 Histogram of mean distribution of organic carbon and hydrocarbon generation potential of mudstone in Jurassic (a); Intersection diagram of peak pyrolysis temperature and hydrogen index of source rocks (b); Diagram of  $R_o$  and depth of source rocks in Shengbei Sub-sag (c)

$J_3q$ —Qigu Formation;  $J_2q$ —Qiketai Formation;  $J_2s$ —Sanjianfang Formation;  $J_2x$ —Xishanyao Formation;  $J_1s$ —Sangonghe Formation;  $J_1b$ —Badaowan Formation

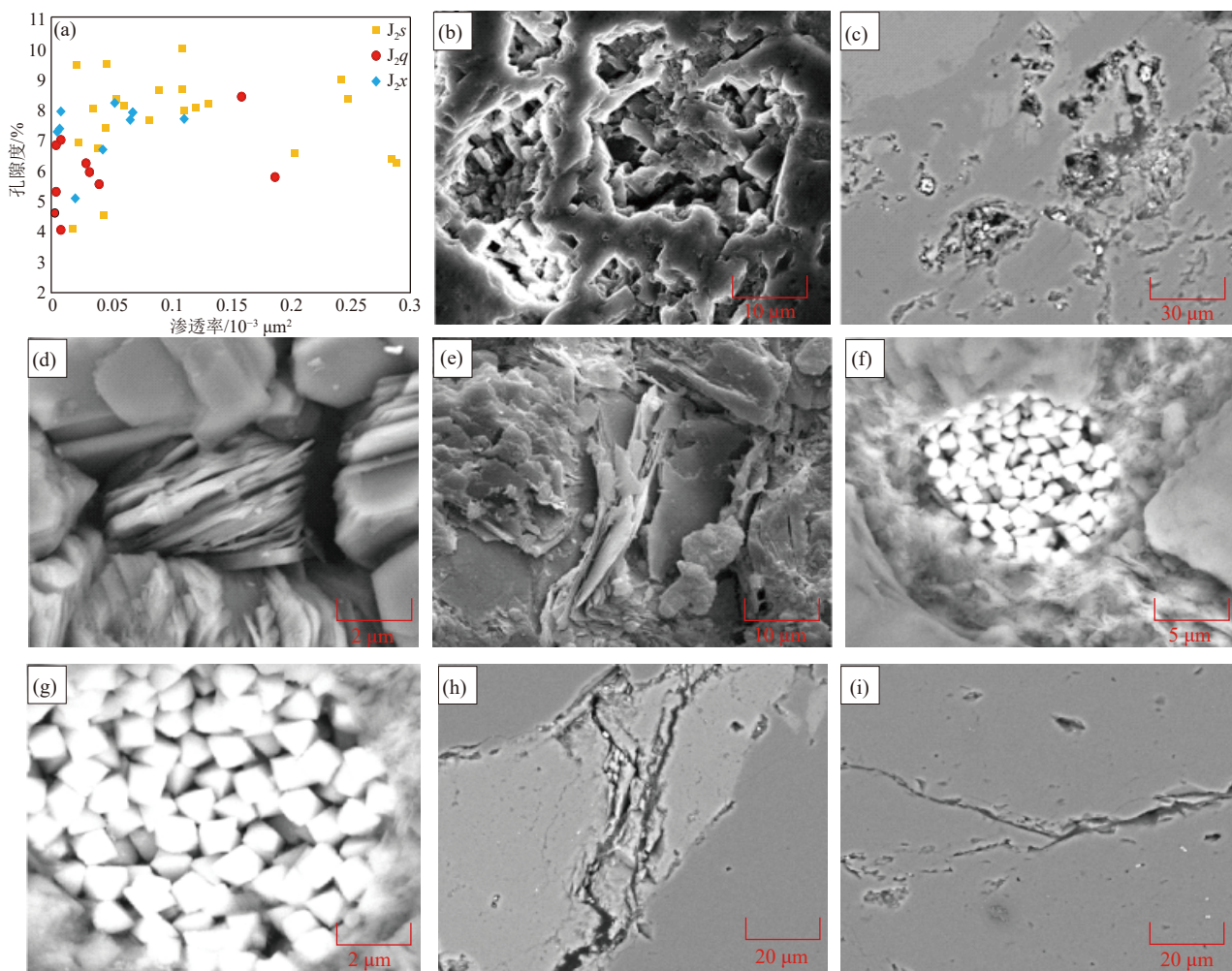


图 4 致密砂岩孔隙度和渗透率关系图 (a)、典型样品扫描电镜分析图 (b~i)

J<sub>2q</sub>—七克台组; J<sub>2s</sub>—三间房组; J<sub>2x</sub>—西山窑组; b—胜北 5 井, J<sub>2q</sub>, 4002.13 m, 灰色细砂岩, 长石粒内溶蚀孔; c—台参 2 井, J<sub>2s</sub>, 4481.84 m, 含粒不等粒砂岩, 长石粒内溶蚀孔; d—胜北 10 井, J<sub>2s</sub>, 3900.00 m, 灰色荧光砂岩, 黏土矿物层间孔; e—连北 5 井, J<sub>2s</sub>, 3896.23 m, 灰色细砂岩, 黏土矿物层间孔; f—连砂 1 井, J<sub>2x</sub>, 3764.44 m, 灰色砂岩, 黄铁矿晶间孔; g—连砂 1 井, J<sub>2x</sub>, 3764.44 m, 灰色砂岩, 黄铁矿晶间孔; h—胜北 5 井, J<sub>2q</sub>, 4002.13 m, 灰色细砂岩, 颗粒内微裂缝; i—台参 2 井, J<sub>2s</sub>, 4481.84 m, 浅灰色荧光含粒不等粒砂岩, 微裂缝

Fig.4 The relationship between porosity and permeability of tight sandstone (a), SEM analysis of typical samples (b~i)  
J<sub>2q</sub>—Qiketai Formation; J<sub>2s</sub>—Sanjianfang Formation; J<sub>2x</sub>—Xishanyao Formation; b—Well Shengbei 5, J<sub>2q</sub>—4002.13 m, gray fine sandstone, dissolution pores in feldspar grains; c—Well Taican 2, J<sub>2s</sub>, 4481.84 m, granule-bearing anisometric sandstone, dissolution pores in feldspar grains; d—Well Shengbei 10, J<sub>2s</sub>, 3900.00 m, gray fluorescent sandstone, clay mineral interbedded pores; e—Well Lianbei 5, J<sub>2s</sub>, 3896.23 m, gray fine sandstone with clay mineral interbedded pores; f—Well Liansha 1, J<sub>2x</sub>, 3764.44 m, gray sandstone, pyrite intercrysalline pores; g—Well Liansha 1, J<sub>2x</sub>, 3764.44 m, gray sandstone, pyrite intercrysalline pores; h—Well Shengbei 5, J<sub>2q</sub>, 4002.13 m, fine gray sandstone with microfractures in the grain; i—Well Taican 2, J<sub>2s</sub>, 4481.84 m, light gray fluorescent granulated anisometric sandstone, microfracture

$0.111 \times 10^{-3} \mu\text{m}^2$ 。

扫描电镜观测结果显示砂岩储层孔隙类型以次生溶蚀孔为主, 同时发育黏土矿物层间孔、黄铁矿晶间孔和微裂缝。石英、长石等遭遇不同程度的溶蚀形成海绵状的粒内溶蚀孔在研究区分布较广(图 4b、c)。矿物颗粒内部层间孔在致密储层内也较发育, 这种层间孔可能是蒙脱石与高岭石等黏土矿物在成岩过程中的转化和交代作用而形成的

(图 4d、e)。同时致密砂岩储层内还观测到发育于草莓状黄铁矿内部的晶间孔(图 4f、g)和多被黏土矿物充填的微裂缝(图 4h、i)。

## 4 压力系统发育特征

### 4.1 超压测井响应与单井预测

实测压力数据(图 5a、b)显示研究区发育超压, 超压压力系数主要分布在 1.2~1.6。利用泥岩的(声

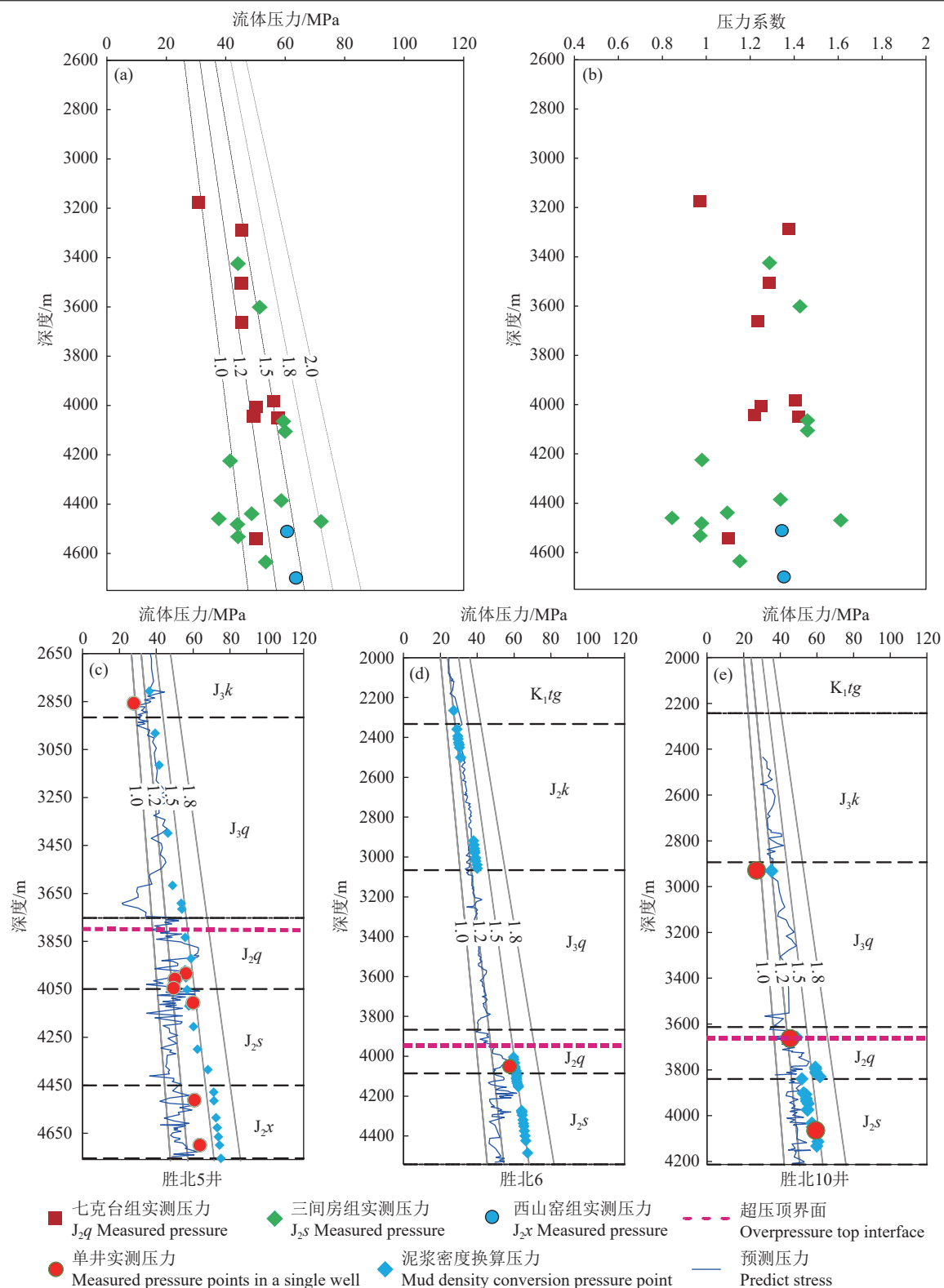


图 5 胜北洼陷中侏罗统实测地层压力对比

 $K_1tg$ —吐谷鲁群;  $J_3k$ —喀拉扎组;  $J_3q$ —齐古组;  $J_2q$ —七克台组;  $J_2s$ —三间房组;  $J_2x$ —西山窑组

Fig. 5 Comparison of Middle Jurassic measured formation pressure, Shengbei Sub-sag

 $K_1tg$ —Tugulu group;  $J_3k$ —Kalazha Formation;  $J_3q$ —Qigu Formation;  $J_2q$ —Qiketai Formation;  $J_2s$ —Sanjianfang Formation;  $J_2x$ —Xishanyao Formation

波、电阻率等)测井曲线、泥浆数据和实测地层压力数据对比分析,对超压具有明显响应特征的主要有声波、密度和电阻率测井曲线。其中声波测井曲线偏离正常趋势线明显,响应特征最明显。

基于 Eaton 法的基本原理,利用实测声波测井曲线值偏离正常压力条件下测井曲线趋势线的程度(Bowers, 1995; Shi et al., 2013; 罗胜元等, 2015),对研究区探井的地层压力进行预测,取得很好的应用效果。具体流程:首先挑选泥岩正常压实情况下的声波时差,并计算正常压实情况下压力随深度的变化规律;当超压发育时,声波时差偏离正常趋势线,超压发育的大小与偏离程度呈一定的关系。通过对研究区单井测井曲线变化规律的分析,利用 Eaton 公式,对研究区单井地层压力进行预测。

典型单井(图 5c~e)揭示单井超压发育,压力系数集中在 1.2~1.5,极少地层超过 1.5。通过实测压力与预测压力对比分析,预测结果与实测结果吻合较好(图 6)。单井纵向压力分布特征表明七克台组中上部至少存在一个压力封存箱;三间房组上部至少存在一个压力封存箱;西山窑组中下部至少存在一个压力封存箱。

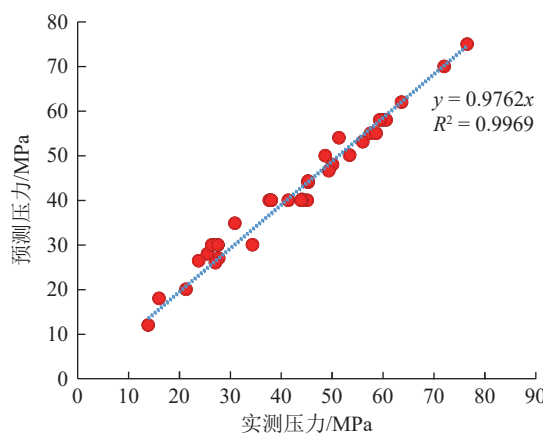


图 6 实测压力与预测压力结果对比

Fig.6 Comparison of measured pressure and predicted pressure results

#### 4.2 超压顶界面

通过超压顶界面连井对比(图 7)揭示超压顶界面主要发育在七克台组中上部。超压顶界面分布深度范围不均一,不同区域深度差异较大,并且在超压顶界面上部附近发育一套较厚泥质沉积,对超

压起到明显的封盖作用,有利于超压保存。

#### 4.3 超压平面发育特征

利用速度谱资料,对七克台组、三间房组和西山窑组地层压力系数进行预测(图 8)。七克台组、三间房组和西山窑组超压发育明显受断裂控制,研究区东部近南北向区域大断裂东边发育超压或强超压。东南部超压强度大于北部。同时,西北角发育超压,随着埋深增加,超压强度增强。在胜北 26 井附近与区域大断裂伴生强超压,随着埋深增加,超压强度不断减小。

### 5 超压成因与油气成藏

#### 5.1 超压成因

Bowers(1995)将水热增压、生烃作用、压力传导、蒙脱石脱水等增压机制统称为流体膨胀作用,最终将产生异常高压的原因归结为两个:不均衡压实和流体膨胀(Bowers, 1995; Wang et al., 2019)。正常压实作用过程中,随着地层沉降并正常压实,岩石骨架颗粒间的有效应力增大,同时孔隙度相应减小、岩石密度增大,所有经历正常压实的地层孔隙度都应该沿着一条初始曲线规律性地变化。在土力学中,当有效应力持续增加时,有效应力-孔隙度变化关系称为原始加载曲线,有效应力减小时则称为卸载曲线。当发生不均衡压实作用时,孔隙流体不能被正常排出,阻碍了固体颗粒间的接触,并部分承担了上覆岩层压力,使固体颗粒间有效应力相应减小。如果所有孔隙流体都被“滞留”,孔隙度将保持常量,压实作用停止,有效应力也将不再随深度变化,因此地层将在加载曲线上某点“滞留”,不会脱离加载曲线。在沉积物埋藏过程中,加、卸载条件下有效应力-孔隙度关系的差异,是区分超压成因、预测超压大小的基础(Bowers, 1995; 罗胜元等, 2015; Liu et al., 2021)。

声波时差测井和密度测井数据的交会图可以用来区分泥岩中超压的不同成因机制,特别是不同的流体膨胀机制和流体传导机制。在正常压力地层,随着埋深的增加压力按照正常的趋势压实,在交会图上落于加载曲线上,密度和声波速度随着深度的增加都有所增大。不同成因引起超压在声波和密度交汇图上有显著的特征。欠压实引起的超压地层与正常压力地层相比,具有相同的孔隙度背

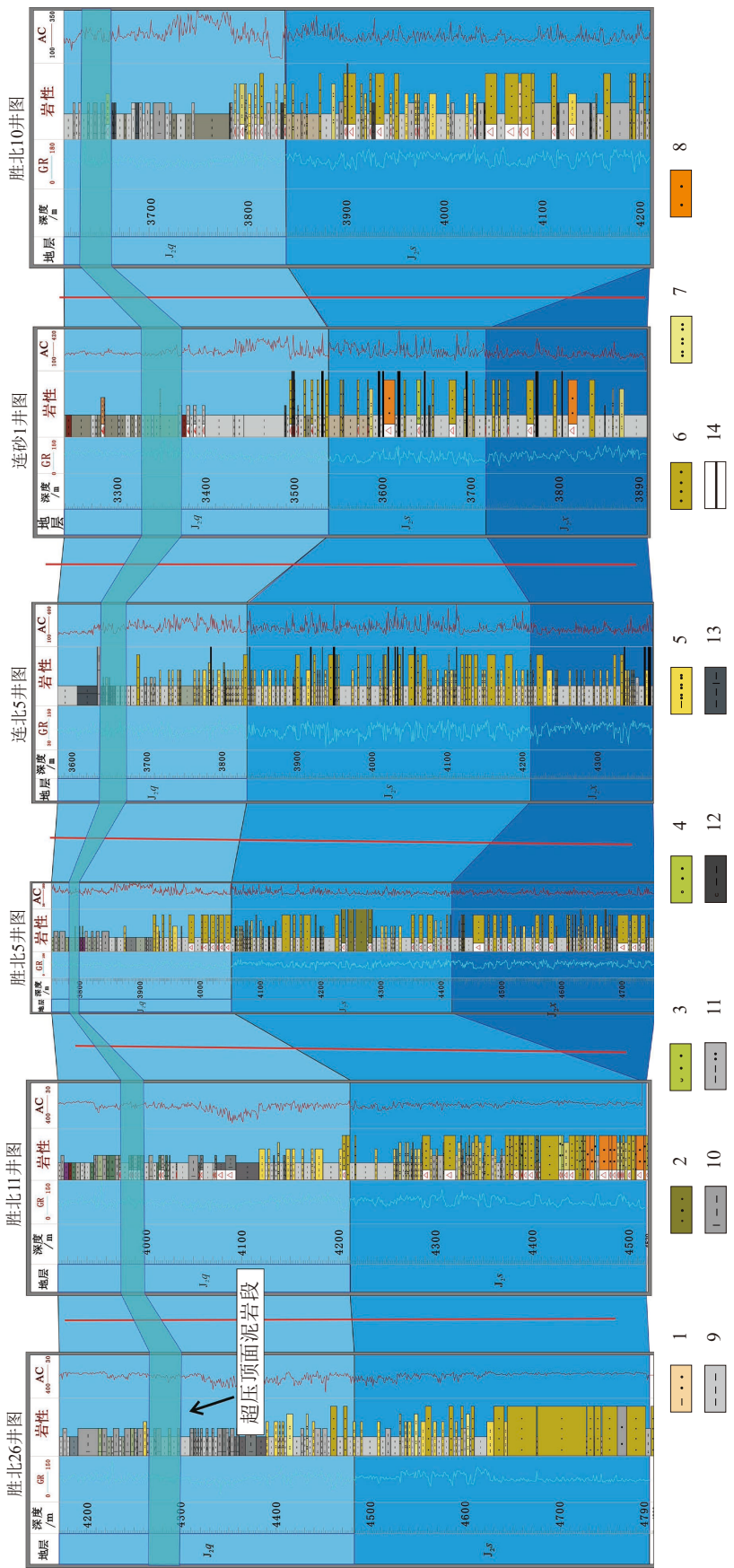


图 7 胜北 26-胜北 11-胜北 5-连北 5-连砂 1-胜北 10 井超压顶面泥岩段连井对比剖面  
1—荧光泥质砂岩; 2—砂砾岩; 3—砾状砂岩; 4—荧光粒状砂岩; 5—泥质粉砂岩; 6—泥质粉砂岩; 7—细砂岩; 8—粗砂岩; 9—粗砂岩; 10—灰质泥岩; 11—粉砂质泥岩; 12—黑色碳质泥岩;  
13—灰色含灰泥岩; 14—黑色煤  
Fig.7 Well Shengbei 26-Shengbei 11-Shengbei 1-Well Lianbei 5-Liansha 1-Well Shengbei 10 overpressure top mudstone section comparison profile  
1-Fluorescent argillaceous sandstone; 2-Gluteinite; 3-Granular sandstone; 4-Fluorescent granular sandstone; 5-Muddy siltstone; 6-Siltstone; 7-Fine sandstone; 8-Coarse sandstone;  
9-Grey mudstone; 10-Lime mudstone; 11-Lime mudstone; 12-Black carbonaceous mudstone; 13-Grey lime mudstone; 14-Black coal

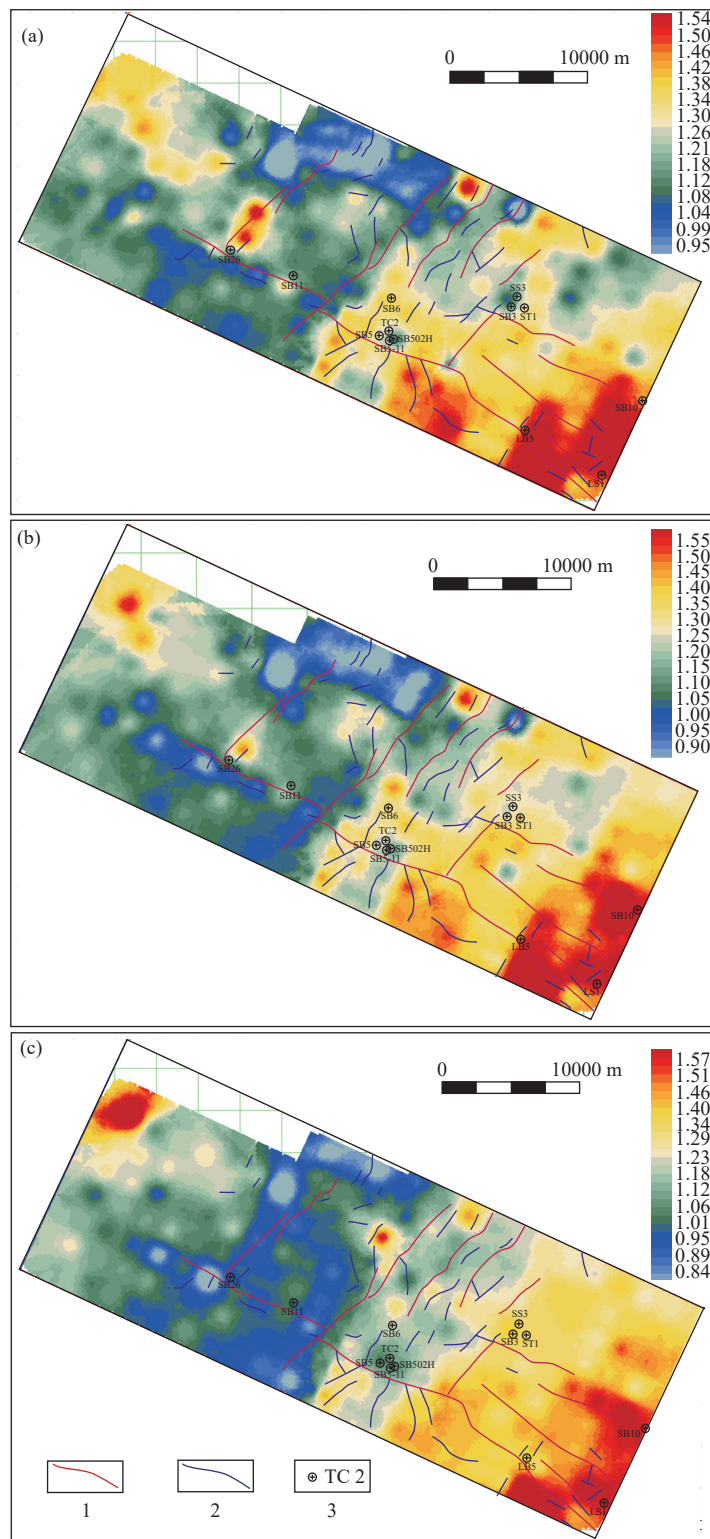


图 8 七克台组 (a)、三间房组 (b)、西山窑组 (c) 地层压力系数预测与断裂分布叠合图  
1—区域大断裂; 2—小断裂; 3—井位与井名

Fig.8 Prediction of formation pressure coefficient and superimposition of fault distribution of Qiketai Formation (a), Sanjianfang Formation (b), Xishanyao Formation (c)  
1—Regional large fault; 2—Small fault; 3—Well location and name

景下的密度和声波时差,交汇点处于加载曲线上;生气作用引起的超压,对地层密度的影响不大,但是由于超压引起有效应力减小使声波速度有明显的降低;由于上覆压力传导或者是泥岩的成岩作用引起的超压,使得密度增加,而声波速度只有较小或者几乎无变化。成岩和负荷传导作用混合成因的超压,导致密度增加和声波速度降低(图 9a)。

密度和声波速度测受岩性影响极大,通常选取泥岩的测井资料进行超压成因分析。泥岩的密度-声波速度交汇图(图 9b)显示极少的泥岩测井数据交汇点分布在正常压实地层的加载趋势线上,少量交汇点分布于成岩作用线上,绝大多数点分布于压力传导趋势线附近。结合研究区勘探认识,超压成因为下部地层压力传导和生烃增压。

## 5.2 致密储层成藏期次

勘探成果和前人研究结果表明胜北洼陷发育中一下侏罗统七克台组、水西沟群烃源岩和中二叠统桃东沟群烃源岩(Wang et al., 2015; Wang et al., 2018; 荀红光等, 2019; Feng et al., 2020; 李天军等, 2021; 吴琰杰等, 2021)。基于地层、岩性和大地热流等资料,结合实测镜质体反射率数据,利用 BasinMod 盆地模拟软件对研究区典型探井进行单井模拟(图 10b),结果表明中侏罗世以来七克台组、三间房组、西山窑组和八道湾组一直发生构造沉降作用:中侏罗世时期中下侏罗统发生快速构造沉降,沉降速度较快,直至晚侏罗世,早白垩世时期,沉降速度急剧变慢,至中晚白垩世时期,沉降速度

再次变缓,直至古新世以后,发生快速沉降,沉降速度增大。

中二叠世以来,桃东沟群( $P_2td$ )一直发生构造沉积作用:中二叠世时期桃东沟群( $P_2td$ )发生快速沉降,沉降速度较快,直至早侏罗世;早中侏罗世时期,沉降速度降低;晚侏罗世至早白垩世时期,沉积速度增大,快速沉降;晚侏罗世至古近世时期,沉积速度减低,缓慢沉降,古新世以后沉降速度再次增大。

中二叠统桃东沟群烃源岩在晚三叠世开始生烃,晚侏罗世达到生烃高峰;中一下侏罗统水西沟群烃源岩在中侏罗世时期开始生烃,在晚侏罗世末至早白垩世达到生烃高峰;七克台组烃源岩在晚侏罗世开始生烃,晚白垩世至今处于生烃高峰期。

典型探井包裹体样品(胜深 3 井, 4453.71 m; 连北 5 井, 4122.65 m; 等)(图 10a)显示中下侏罗统储层中发育气液两相包裹体、纯气相包裹体、含烃盐水包裹体。流体包裹体显微测温和热埋藏史投点结果揭示天然气充注持续时间较长:从晚侏罗世—古新世至今,主要成藏期次为晚侏罗世至早白垩世和古新世至今。

## 5.3 成藏模式

胜北洼陷中侏罗统致密气藏以“远源—近源两期成藏、压力—断裂协同输导、断裂—超压协调控制”的模式为主。具体表现为(图 11):

烃源岩评价和勘探成果表明研究区发育中一下侏罗统七克台组烃源岩和水西沟群烃源岩,对于

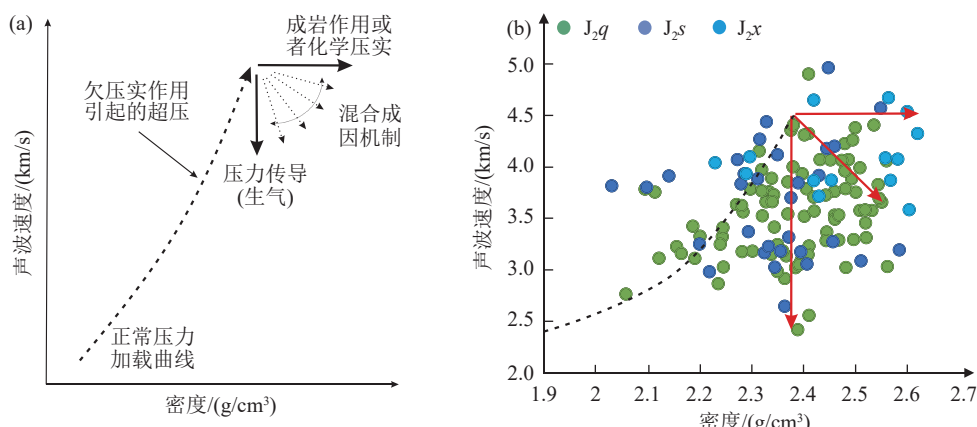


图 9 超压成因机制判定模板 (a)、研究区超压成因判定 (b)(图例释义见图 3)

Fig.9 Overpressure cause mechanism determination template (a), overpressure cause determination diagram (b) in the study area (see Fig.3 for illustration)

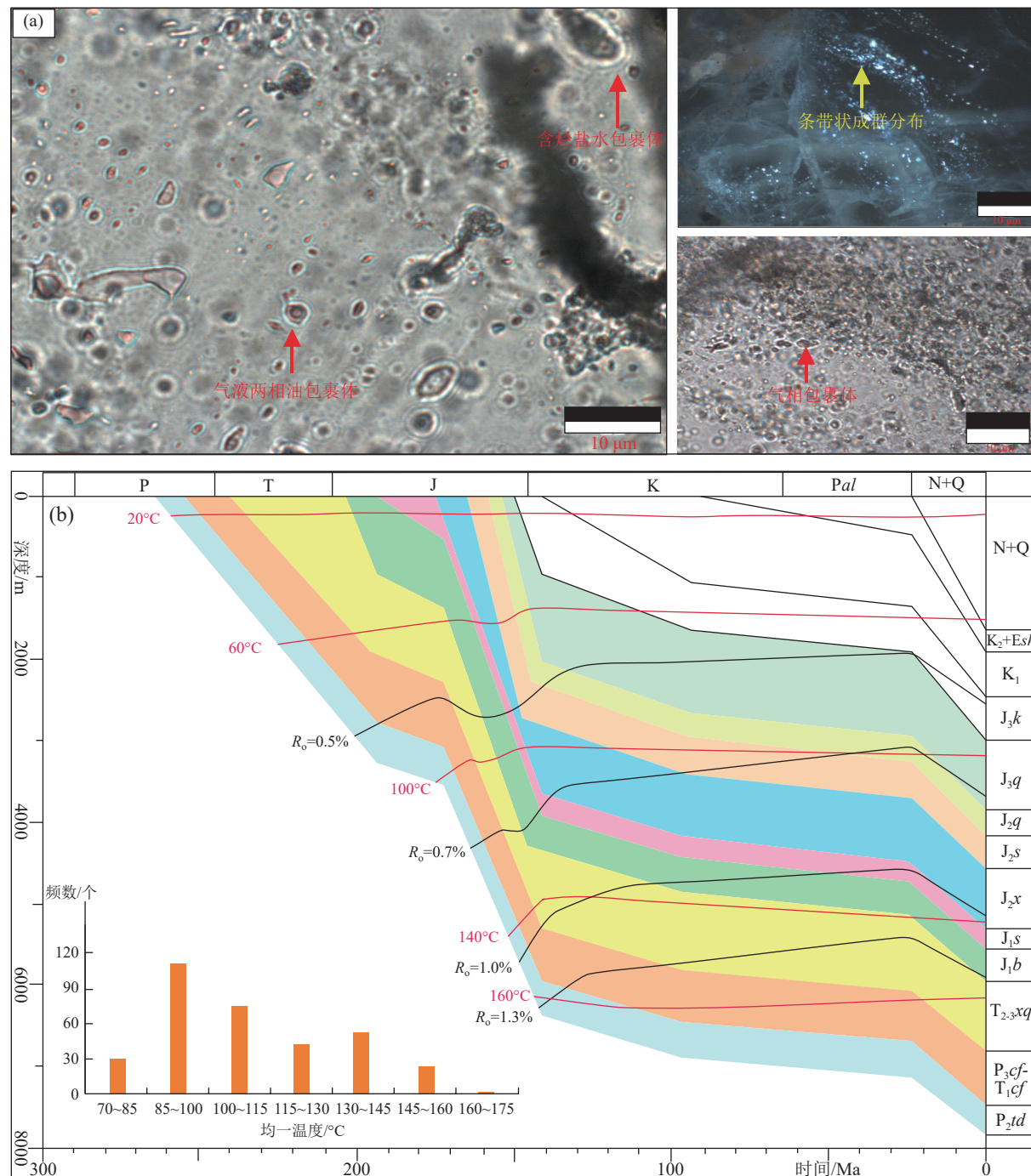


图 10 中侏罗统典型样品包裹体识别与均一温度分布 (a)、台参 2 井热演化、温度与埋藏史模拟图 (b)  
P—二叠系; T—三叠系; J—侏罗系; K—白垩系; Pal—古近系; N+Q—新近系+第四系; K<sub>2</sub>+Esh—上白垩系+鄯善群; K<sub>1</sub>—下白垩统; J<sub>3</sub>k—喀拉扎组; J<sub>3</sub>q—齐古组; J<sub>2</sub>q—七克台组; J<sub>2</sub>s—三间房组; J<sub>2</sub>x—西山窑组; J<sub>1</sub>s—三工河组; J<sub>1</sub>b—八道湾组; T<sub>2-3</sub>xq—小泉沟群; P<sub>3</sub>cf-T<sub>1</sub>cf—上-下苍房沟群; P<sub>2</sub>td—桃东沟群

Fig.10 Inclusion identification and homogenization temperature distribution of typical Middle Jurassic samples(a), simulation diagram of thermal evolution, temperature and burial history of Well Taican 2 (b)  
P-Permian; T-Triassic; J-Jurassic; K-Cretaceous; Pal-Paleocene; N+Q-Neogene+Quaternary; K<sub>2</sub>+Esh-Upper Cretaceous+Shanshan Group; K<sub>1</sub>-Lower Cretaceous; J<sub>3</sub>k-Kalazha Group; J<sub>3</sub>q-Qigou Formation; J<sub>2</sub>q-Qiketai Formation; J<sub>2</sub>s-Sanjianfang Formation; J<sub>2</sub>x-Xishanyao Formation; J<sub>1</sub>s-Sangonghe Formation; J<sub>1</sub>b-Badaowan Formation; T<sub>2-3</sub>xq-Xiaoquangou Group; P<sub>3</sub>cf-T<sub>1</sub>cf-Upper-Lower Cangfanggou Group; P<sub>2</sub>td-Taodonggou Group

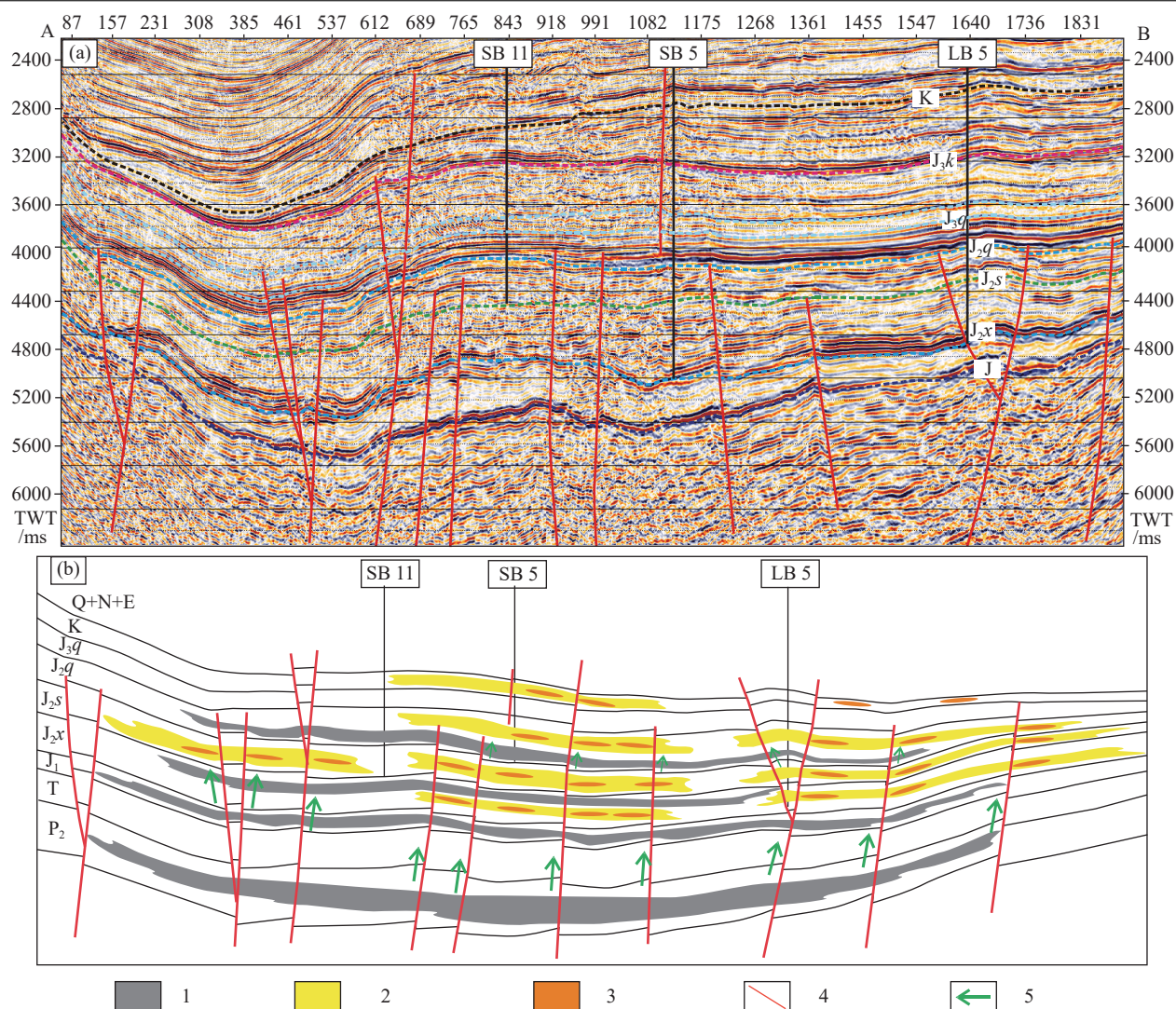


图 11 胜北洼陷近东西向典型地震剖面解释图(a)、胜北洼陷中侏罗统致密气成藏模式图(b)  
1—原岩; 2—砂体; 3—甜点; 4—断层; 5—压力传导方向; K—白垩系; J<sub>3</sub>k—喀拉扎组; J<sub>3</sub>q—齐古组; J<sub>2</sub>q—七克台组; J<sub>2</sub>s—三间房组; J<sub>2</sub>x—西山窑组; J—侏罗系

Fig.11 Interpretation of typical near E–W seismic profiles(a), model diagram of tight gas accumulation in middle Jurassic in Shengbei Sub-sag of Turpan–Hami Basin(b)  
1—Original rock; 2—Sand body; 3—Sweet spot; 4—Fault; 5—Pressure transmission direction; K—Cretaceous; J<sub>3</sub>k—Kalazha Formation; J<sub>3</sub>q—Qigu Formation; J<sub>2</sub>q—Qiketai Formation; J<sub>2</sub>s—Sanjianfang Formation; J<sub>2</sub>x—Xishanyao Formation; J—Jurassic

中侏罗统致密砂岩气藏属于近源成藏;同时中二叠统桃东沟群为主力烃源岩之一,为远源成藏。包裹体均一温度揭示天然气充注存在至少两个主要期次,分别为晚侏罗世至早白垩世和古新世至今。

近东西向地震解释剖面揭示研究区发育多条沟通侏罗系与二叠系和基底的大断裂(图 11a),这些大断裂实现了中侏罗统致密储层与下部水西沟群和桃东沟群烃源岩的连通,为致密砂岩储层远源成藏提供了运移通道。伴随烃类的运移,下部地层

压力传导至上部中侏罗统,同时七克台组烃源岩生烃增压,共同控制中侏罗统超压发育。

断裂系统与烃源岩、砂体和致密气藏甜点区相连,压力传导和生烃形成超压,超压为天然气运移与聚集成藏提供动力,合理的源储空间配置、断裂系统与超压发育协同控制着致密气成藏。

## 6 结 论

(1) 胜北洼陷探井揭示中下侏罗统七克台组、

西山窑组、三工河组和八道湾组烃源岩丰度较高, 有机质类型以 III 型干酪根为主, 整体处于成熟期, 以生气为主。中侏罗统发育低孔低渗—特低渗致密储层, 孔隙类型以次生溶蚀孔为主, 同时发育黏土矿物层间孔、黄铁矿晶间孔和微裂缝。

(2) 中侏罗统发育超压, 压力系数主要分布在 1.2~1.5, 纵向上超压顶界面位于七克台组中上部, 平面上超压主要分布在胜北洼陷东部或者东南部, 超压分布受断裂系统控制。七克台组、三间房组和西山窑组都至少发育一个超压封存箱。超压成因为压力传导和生烃增压。

(3) 胜北洼陷烃源岩排烃时间持续较长, 从晚三叠世至今。两期主要成藏期次为: 晚侏罗世至早白垩世和古新世至今。中侏罗统致密气藏以“远源—近源两期成藏、压力—断裂协同输导、断裂—超压协调控制”的模式为主。

## References

- Bowers G L. 1995. Pore-pressure estimation from velocity data: Accounting for overpressure mechanisms besides undercompaction[J]. *SPE Drilling and Completion*, 10(2): 89–95.
- Cao Hua, Gong Jingjing, Wang Guifeng. 2006. The cause of overpressure and its relationship with reservoir forming[J]. *Natural Gas Geoscience*, 17(3): 422–425 (in Chinese with English abstract).
- Feng Y, Huang Z L, Wang E Z, Zhang H, Li T J, Liang Y. 2020. The hydrocarbon generation and expulsion features of source rocks and tight oil potential of the second member of the Qiketai Formation, Shengbei area in the Turpan–Hami Basin, NW China[J]. *Geological Journal*, 56(1): 337–358.
- Gou Hongguang, Zhang Pin, She Jiachao, Wang Zhiyong, Lin Lin, Zhang Yiting. 2019. Petroleum geological conditions, resource potential and exploration direction in Turpan–Hami Basin[J]. *Marine Origin Petroleum Geology*, 24(2): 85–96 (in Chinese with English abstract).
- Hao Aisheng, Li Jian, Guo Jianying, Wu Hao, Ran Qigui, Li Zhisheng, Qi Xuening, Zhang Lu, Wang Xiaobo. 2021. Characteristics and exploration direction of tight sandstone gas reservoirs in the Lower Jurassic of Turpan–Hami Basin[J]. *Natural Gas Geoscience*, 32(8): 1212–1222 (in Chinese with English abstract).
- Hua Y Q, Guo X W, Tao Z, He S, Dong T, Han Y J, Yang R. 2021. Mechanisms for overpressure generation in the Bonan sag of Zhanhua depression, Bohai Bay Basin, China[J]. *Marine and Petroleum Geology*, 128: 105032.
- Li Hongzhe, Yang Zhanlong, Wu Qingpeng, Wan Chuanzhi. 2006. The Application of sedimentary facies analyses in lithologic pool—Taking Turpan–Hami Basin Jurassic serious and Cretaceous serious as examples[J]. *Natural Gas Geoscience*, 17(5): 698–702 (in Chinese with English abstract).
- Li S L, Ma Y Z, Gomez E. 2021. Importance of modeling heterogeneities and correlation in reservoir properties in unconventional formations: Examples of tight gas reservoirs[J]. *Journal of Earth Science*, 32(4): 809–817.
- Li Tianjun, Huang Zhilong, Zhang Yiting, Wang Rui, Zhang Hua, Zhou Zaihua. 2021. Lithofacies characteristics and genetic model of shallow lacustrine fine-grained sediments and its geological significance for shale oil in the Qiketai Formation in the Shengbei subsag, Turpan–Hami basin[J]. *Acta Geologica Sinica*, 95(12): 3869–3884 (in Chinese with English abstract).
- Li W, Chen Z X, Huang P H, Yu Z C, Min L, Lu X S. 2021. Formation of overpressure system and its relationship with the distribution of large gas fields in typical foreland basins in central and western China[J]. *Petroleum Exploration and Development*, 48(3): 625–640.
- Li Zaiguang, Yang Zhanlong, Li Hongzhe, Guo Jingyi, Huang Yunfeng, Wu Qingpeng. 2006. Detection of hydrocarbon potentials in Shengbei area of Tuha Basin[J]. *Natural Gas Geoscience*, 17(4): 532–537 (in Chinese with English abstract).
- Li Zaiguang, Yang Zhanlong, Li Lin, Guo Jingyi, Huang Yunfeng, Wu Qingpeng, Li Hongzhe. 2006. Hydrocarbon distribution of Shengbei area[J]. *Natural Gas Geoscience*, 17(1): 94–96 (in Chinese with English abstract).
- Liu B, Huang Z L, Tu X X, Zhang J X, Mu K X. 2011. Structural styles and hydrocarbon accumulation of the northern piedmont belt in the Taihei Sag, Turpan–Hami Basin[J]. *Petroleum Exploration and Development Online*, 38(2): 152–158.
- Liu Jiangtao, Huang Zhilong, Wang Hai. 2021. Dominant control factors of hydrocarbon distance accumulating in western arc-like zone of Turpan–hami Basin[J]. *Journal of China University of Petroleum(Edition of Natural Science)*, 34(2): 24–30 (in Chinese with English abstract).
- Liu Y K, He Z L, He S, Zhang D W, Li T Y, Wang X L. 2021. A new quantitative model and application for overpressure prediction in carbonate formation[J]. *Journal of Petroleum Science and Engineering*, 198: 108145.
- Luo Shengyuan, He Sheng, Jin Qiuyue, Yang Ruizhi, Zhang Junli. 2015. Overpressure system classification and structure characteristic in Bonan Sag[J]. *Journal of Jilin University(Earth Science Edition)*, 45(1): 37–51 (in Chinese with English abstract).
- Shi W Z, Xie Y H, Wang Z F, Li X S, Tong C X. 2013. Characteristics of overpressure distribution and its implication for hydrocarbon exploration in the Qiongdongnan Basin[J]. *Journal of Asian Earth Sciences*, 66(8): 150–165.
- Tang Wenbin, Xu Shenglin, Chen Hongde, Chen Anqing, Liang Jie, Xiao Dongsheng. 2017. Discovery of seismites in the first member

- of the Kelaza Formation in central Taipei Sag of Tuha Basin and its geological significance[J]. *Oil & Gas Geology*, 38(2): 345–354 (in Chinese with English abstract).
- Wang Jinsong, Wang Hua, Liang Shijun, Huang Weidong, Lü Xueju. 2009. Analysis on exploration of natural gas in the Turpan–Hami Basin[J]. *Petroleum Geology & Experiment*, 31(4): 333–337 (in Chinese with English abstract).
- Wang Peng, Sun Linghui, Wang He, Li Zi'an. 2020. Microscopic pore structure of Ahe tight sand gas reservoirs of the Low Jurassic in Kuqa Depression and its controls on tight gas enrichment[J]. *Oil & Gas Geology*, 41(2): 295–304 (in Chinese with English abstract).
- Wang W , Lu S F, Chen X, Li X W, Li J J, Tian W C. 2015. A new method for grading and assessing the potential of tight sand gas resources: A case study of the Lower Jurassic Shuixigou Group in the Turpan–Hami Basin, NW China[J]. *Petroleum Exploration and Development Online*, 42(1): 66–73.
- Wang Y P, Zou Y R, Zhan Z W, Lin X H, Liang T. 2018. Origin of natural gas in the Turpan–Hami Basin, NW China: Evidence from pyrolytic simulation experiment[J]. *International Journal of Coal Geology*, 195: 238–249.
- Wang X, He S, Stuart J. Jones, Yang R, Wei A, Liu C H, Liu Q, Cheng C Y, Liu W M. 2019. Overpressure and its positive effect in deep sandstone reservoir quality of Bozhong Depression, offshore Bohai Bay Basin, China[J]. *Journal of Petroleum Science and Engineering*, 182: 106362.
- Wu Yanjie, Wang shuai, He Lei, Wang Zidi, Nie Guoquan. 2021. Research on the burial history and the thermal evolution history of the Jurassic coal-measure source rocks in the eastern margin of Xiaocaohu Sag[J]. *Northwestern Geology*, 54(4): 180–191 (in Chinese with English abstract).
- Yang Zhanlong, Chen Qilin, Guo Jingyi. 2005. The particularity analysis of stratigraphy reservoirs in Shengbei depression[J]. *Natural Gas Geoscience*, 16(2): 181–185, 189 (in Chinese with English abstract).
- Zeng Fancheng, Zhang Changmin, Li Zhongcheng, Zhang Guoyi, Zhang Chi, Wang Yongjun, Sun Wentie, Deng Qingjie. 2021. Blocky pyroclastic rocks in the Cretaceous Shahezi Formation in Wangfu gas field, southern Songliao Basin[J]. *Oil & Gas Geology*, 42(2): 481–493 (in Chinese with English abstract).
- Zhao H J, Zhang M, Wang Z Y. 2010. Geochemical characteristics and possible origin of natural gas in the Taipei Depression, Turpan–Hami Basin, China[J]. *Chinese Journal of Geochemistry*, 29(3): 307–312.
- Zhao Jingzhou, Li Jun, Cao Qing, Bai Yubin, Er Chuang, Wang Xiaomei, Xiao Hui, Wu Weitao. 2013. Hydrocarbon accumulation patterns of large tight oil and gas fields[J]. *Oil & Gas Geology*, 34(5): 573–583 (in Chinese with English abstract).
- Zhan Pin, Gou Hongguang, Long Fei, She Jiachao, Wang Zhiyong, Jin Yin. 2018. Natural gas geological conditions, resource potential and exploration direction in Turpan–Hami Basin[J]. *Natural Gas Geoscience*, 29(10): 1531–1541 (in Chinese with English abstract).
- ### 附中文参考文献
- 曹华, 龚晶晶, 汪贵锋. 2006. 超压的成因及其与油气成藏的关系[J]. *天然气地球科学*, 17(3): 422–425.
- 苟红光, 张品, 余家朝, 王志勇, 林霖, 张亦婷. 2019. 吐哈盆地石油地质条件、资源潜力及勘探方向[J]. *海相油气地质*, 24(2): 85–96.
- 郝爱胜, 李剑, 国建英, 吴浩, 冉启贵, 李志生, 齐雪宁, 张璐, 王晓波. 2021. 吐哈盆地侏罗统致密砂岩气藏特征与勘探方向[J]. *天然气地球科学*, 32(8): 1212–1222.
- 李红哲, 杨占龙, 吴青鹏, 万传治. 2006. 沉积相分析在岩性油气藏勘探中的应用——以吐哈盆地胜北洼陷中侏罗统—白垩系为例[J]. *天然气地球科学*, 17(5): 698–702.
- 李在光, 杨占龙, 李红哲, 郭精义, 黄云峰, 吴青鹏. 2006a. 吐哈盆地胜北地区含油性检测[J]. *天然气地球科学*, 17(4): 532–537.
- 李在光, 杨占龙, 李琳, 郭精义, 黄云峰, 吴青鹏, 李红哲. 2006b. 胜北地区油气分布规律[J]. *天然气地球科学*, 17(1): 94–96.
- 李天军, 黄志龙, 张亦婷, 王瑞, 张华, 周在华. 2021. 吐哈盆地胜北洼陷七克台组浅水湖相细粒沉积岩岩相特征、成因模式及页岩油意义[J]. *地质学报*, 95(12): 3869–3884.
- 刘江涛, 黄志龙, 王海. 2010. 吐哈盆地西部弧形带油气远距离运移成藏主控因素[J]. *中国石油大学学报(自然科学版)*, 34(2): 24–30.
- 罗胜元, 何生, 金秋月, 杨睿之, 张君立. 2015. 渤南洼陷超压系统划分及结构特征[J]. *吉林大学学报(地球科学版)*, 45(1): 37–51.
- 唐文斌, 徐胜林, 陈洪德, 陈安清, 梁杰, 肖冬生. 2017. 吐哈盆地台北凹陷中部地区喀拉扎组一段震积岩的发现及其地质意义[J]. *石油与天然气地质*, 38(2): 345–354.
- 王劲松, 王华, 梁世君, 黄卫东, 吕学菊. 2009. 吐哈盆地天然气勘探潜力分析[J]. *石油实验地质*, 31(4): 333–337.
- 王朋, 孙灵辉, 王核, 李自安. 2020. 库车坳陷下侏罗统阿合组致密砂岩储层孔隙微观结构特征及其对致密气富集的控制作用[J]. *石油与天然气地质*, 41(2): 295–304.
- 吴琰杰, 王帅, 何磊, 王紫笛, 聂国权. 2021. 吐哈盆地小草湖凹陷东缘侏罗系煤系烃源岩埋藏史、热演化史模拟[J]. *西北地质*, 54(4): 180–191.
- 杨占龙, 陈启林, 郭精义. 2005. 胜北洼陷岩性油气藏成藏条件特殊性分析[J]. *天然气地球科学*, 16(2): 181–185, 189.
- 曾凡成, 张昌民, 李忠诚, 张国一, 张驰, 王拥军, 孙文铁, 邓庆杰. 2021. 断块型沉火山碎屑岩致密气藏有效储层控制因素及分布规律——以松辽盆地南部王府气田白垩系沙河子组为例[J]. *石油与天然气地质*, 42(2): 481–493.
- 赵靖舟, 李军, 曹青, 白玉彬, 耳闻, 王晓梅, 肖晖, 吴伟涛. 2013. 论致密大油气田成藏模式[J]. *石油与天然气地质*, 34(5): 573–583.
- 张品, 苟红光, 龙飞, 余家朝, 王志勇, 金颖. 2018. 吐哈盆地天然气地质条件、资源潜力及勘探方向[J]. *天然气地球科学*, 29(10): 1531–1541.